# Ventilation of the Deep Southern Ocean and Deglacial CO 2 Rise

L. C. Skinner, *et al.*

*Science* **328**, 1147 (2010);
DOI: 10.1126/science.1183627

whereupon a threshold was passed and $M_{12}L_{24}$ was exclusively observed (Fig. 4D). This self-organized criticality is reminiscent of emergent behavior observed in complex systems and patterns arising from a multiplicity of simple interactions, such as the emergence of complex biological structures from simple polypeptides (*30*).

With this example, artificial multicomponent self-assembly edges yet closer to the massive scale of biological self-assembly and provides a synthetically simple system for a deeper mechanistic understanding of emergent behavior.

### References and Notes


1. R. W. Horne, *Virus Structure* (Academic Press, New York, 1974).
2. S. Casjens, *Virus Structure and Assembly* (Jones and Bartlett, Boston, 1985).
3. J. M. Grimes *et al*., *Nature* **395**, 470 (1998).
4. W. R. Wikoff *et al*., *Science* **289**, 2129 (2000).
5. D. L. D. Caspar, A. Klug, *Cold Spring Harbor Symp. Quant. Biol.* **27**, 1 (1962).
6. R. Twarock, *Philos. Trans. R. Soc. London Ser. A* **364**, 3357 (2006).
7. R. W. Saalfrank, A. Stark, K. Peters, H. G. Schnering, *Angew. Chem. Int. Ed. Engl.* **27**, 851 (1988).
8. M. Fujita *et al*., *Nature* **378**, 469 (1995).
9. N. Takeda, K. Umemoto, K. Yamaguchi, M. Fujita, *Nature* **398**, 794 (1999).
10. M. Tominaga *et al*., *Angew. Chem. Int. Ed.* **43**, 5621 (2004).
11. D. L. Caulder, R. E. Powers, T. N. Parac, K. N. Raymond, *Angew. Chem. Int. Ed.* **37**, 1840 (1998).
12. D. L. Caulder, K. N. Raymond, *Acc. Chem. Res.* **32**, 975 (1999).
13. P. J. Stang, B. Olenyuk, D. C. Muddiman, R. D. Smith, *Organometallics* **16**, 3094 (1997).
14. B. Olenyuk, J. A. Whiteford, A. Fechtenkötter, P. J. Stang, *Nature* **398**, 796 (1999).
15. B. Olenyuk, M. D. Levin, J. A. Whiteford, J. E. Shield, P. J. Stang, *J. Am. Chem. Soc.* **121**, 10434 (1999).
16. S. R. Seidel, P. J. Stang, *Acc. Chem. Res.* **35**, 972 (2002).
17. B. F. Abrahams, S. J. Egan, R. Robson, *J. Am. Chem. Soc.* **121**, 3535 (1999).
18. A. Müller, P. Kögerler, A. W. M. Dress, *Coord. Chem. Rev.* **222**, 193 (2001).
19. A. Müller, S. Roy, *Coord. Chem. Rev.* **245**, 153 (2003).
20. M. Eddaoudi *et al*., *J. Am. Chem. Soc.* **123**, 4368 (2001).
21. D. J. Tranchemontagne, Z. Ni, M. O'Keeffe, O. M. Yaghi, *Angew. Chem. Int. Ed.* **47**, 5136 (2008).
22. B. Moulton, J. Lu, A. Mondal, M. J. Zaworotko, *Chem. Commun. (Camb.)* (9): 863 (2001).
23. L. R. MacGillivray, J. L. Atwood, *Nature* **389**, 469 (1997).
24. M. M. Conn, J. Rebek Jr., *Chem. Rev.* **97**, 1647 (1997).
25. K. Suzuki, M. Tominaga, M. Kawano, M. Fujita, *Chem. Commun. (Camb.)* (13): 1638 (2009).
26. S. Sato *et al*., *Science* **313**, 1273 (2006).
27. H. S. M. Coxeter, *Regular Polytopes* (Dover Publications, New York, ed. 3, 1973).
28. P. Bak, C. Tang, K. Wiesenfeld, *Phys. Rev. Lett.* **59**, 381 (1987).
29. N. Krasnogor, S. Gustafson, D. A. Pelta, J. L. Verdegay, Eds., *Systems Self-Assembly: Multidisciplinary Snapshots*, vol. 5 of *Studies in Multidisciplinary Series* (Elsevier, Amsterdam, 2008).
30. H. J. Jensen, *Self-Organized Criticality: Emergent Complex Behavior in Physical and Biological Systems*, Cambridge Lecture Notes in Physics (Cambridge Univ. Press, Cambridge, 2003).
31. Materials, methods, and additional figures are available as supporting material on *Science* Online.
32. K. Yamaguchi, *J. Mass Spectrom.* **38**, 473 (2003).
33. P. Price, *J. Am. Soc. Mass Spectrom.* **2**, 336 (1991).
34. The *Cambridge Crystallographic Data Centre* (CCDC) entry 765717 contains the supplementary crystallographic data for this paper. These data can be obtained free of charge via www.ccdc.cam.ac.uk/conts/retrieving.html (or from the Cambridge Crystallographic Data Centre, 12 Union Road, Cambridge CB2 1EZ, UK; fax: (+44) 1223-336-033; or e-mail: deposit@ccdc.cam.ac.uk).


35. This work was supported by the Japanese Ministry of Education, Culture, Sports, Science and Technology (MEXT) via Grant-in-Aids for Scientific Research on Innovative Areas "Emergence in Chemistry" (20111007) and for Young Scientists (A) (21685007). The experiments of synchrotron x-ray crystallography were performed at the BL38B1 in the SPring-8 with the approval of the Japan Synchrotron Radiation Research Institute (JASRI) (proposal number 2009B1967) and at the NW2A beamline in the advanced ring for pulse x-rays (PF-AR) with the approval of the High Energy Accelerator Research Organization (KEK) (proposal number 2009G502). We thank N. Iwasaki and M. Pelzing (Bruker Daltonics) for the support of CSI-TOF-MS measurements and K. Miura (JASRI) for the support of synchrotron x-ray measurements.


### Supporting Online Material

www.sciencemag.org/cgi/content/full/science.1188605/DC1
Materials and Methods
Figs. S1 to S31
Tables S1 to S4
References

22 February 2010; accepted 13 April 2010
Published online 29 April 2010;
10.1126/science.1188605
Include this information when citing this paper.



# Ventilation of the Deep Southern Ocean and Deglacial $CO_2$ Rise

**L. C. Skinner,[1]* S. Fallon,[2] C. Waelbroeck,[3] E. Michel,[3] S. Barker[4]**

**Past glacial-interglacial increases in the concentration of atmospheric carbon dioxide ($CO_2$) are thought to arise from the rapid release of $CO_2$ sequestered in the deep sea, primarily via the Southern Ocean. Here, we present radiocarbon evidence from the Atlantic sector of the Southern Ocean that strongly supports this hypothesis. We show that during the last glacial period, deep water circulating around Antarctica was more than two times older than today relative to the atmosphere. During deglaciation, the dissipation of this old and presumably $CO_2$-enriched deep water played an important role in the pulsed rise of atmospheric $CO_2$ through its variable influence on the upwelling branch of the Antarctic overturning circulation.**

There is a broad consensus that glacial-interglacial atmospheric carbon dioxide ($CO_2$) change depends primarily on marine processes operating in the Southern Ocean (*1*–*3*). The special importance of this region is suggested by the observed link between atmospheric $CO_2$ and Antarctic temperature change on both orbital and millennial time scales (*4*, *5*). However, the expectation of a Southern Ocean role in past $CO_2$ variability is also based on strong conceptual grounds because this is the region of the global ocean where most deep water makes its first contact with the sea surface (*6*), and consequently where $CO_2$ that has accumulated in the deep sea can be released to the atmosphere.

One important clue regarding the ocean's potential role in atmospheric $CO_2$ variability comes from the record of atmospheric radiocarbon activity ($\Delta^{14}C_{atm}$), which reveals an apparent "excess" of atmospheric $^{14}C$ during the last glacial period relative to the present and relative to concurrent $^{14}C$ production rates (*7*). This apparent $\Delta^{14}C_{atm}$ excess was eliminated across the last deglaciation in two steps (*8*, *9*), each of which coincided with a sharp rise in atmospheric $CO_2$ (*10*) (Fig. 1, vertical lines). The widely held expectation is therefore that lowered glacial $CO_2$ and the rapid deglacial $CO_2$ rise were made possible by the sequestration of an aged, carbon-rich deep-water mass that was mixed with the atmosphere in two pulses across the deglaciation.

Although this expectation, referred to here as the "deep re-coupling hypothesis," is compelling and circumstantially supported (*2*, *11*), it has yet to be confirmed directly through marine $^{14}C$ ventilation reconstructions. For example, available $^{14}C$ evidence from the deep Pacific appears to restrict the putative aged carbon reservoir to depths of >2.8 km in this basin (*8*, *12*). Other marine $^{14}C$ evidence from the North Pacific and North Atlantic suggests at the very least the existence of strong $^{14}C$ activity gradients within the glacial ocean (*9*, *11*, *13*, *14*). The oldest water body thus identified was more than 3000 years offset from the atmosphere (*11*), although its existence and extent during the glacial before ~18 thousand years before the present (ky B.P.) remains unconfirmed. Indeed, none of the available marine $^{14}C$ reconstructions reveal the occurrence of a relatively aged and widely exported deep-water mass before the initiation of the so-

[1]Godwin Laboratory for Palaeoclimate Research, Department of Earth Sciences, University of Cambridge, Downing Street, Cambridge CB2 3EQ, UK. [2]Research School of Earth Sciences, Australian National University (ANU), Canberra ACT 0200, Australia. [3]Laboratoire des Sciences du Climat et l'Environnement/Institut Pierre-Simon Laplace, Laboratoire CNRS-CEA-UVSQ, Bâtiment 12, Avenue de la Terrasse, F-91198, Gif-sur-Yvette Cedex, France. [4]School of Earth and Ocean Sciences, Cardiff University, Cardiff CF10 3YE, UK.

*To whom correspondence should be addressed. E-mail: lcs32@esc.cam.ac.uk

called "mystery interval" [approximately equivalent to Heinrich Stadial 1 (HS1)] at ~17.9 ky B.P., when atmospheric $CO_2$ began to rise and $\Delta^{14}C_{atm}$ began to drop sharply (*8*). Here, we bridge precisely this gap by demonstrating the existence during the last glaciation of a poorly ventilated carbon pool deep in the Atlantic sector of the Southern Ocean that dissipated in two pulses across the deglaciation.

Radiocarbon analyses were performed on paired samples of (monospecific) planktonic and (mixed) benthic foraminifera from core MD07-3076 CQ (44° 4.46'S, 14°12.47'W, 3770 m). All $^{14}C$ samples were subjected to a rigorous cleaning procedure so as to eliminate all adhering phases other than primary carbonate (*15*). Auxiliary Mg/Ca analyses were performed on samples of the planktonic foraminifer species *Globigerina bulloides* and *Neogloboquadrina pachyderma* (left coiling) from the same core (*15*).

The site of MD07-3076 (fig. S1) currently lies on the locus of water that is spread throughout the ocean via upper-ocean and abyssal circulation limbs (*15*). It is expected that this site experienced less North Atlantic Deep Water (NADW) influence during the last glaciation, such as in the deep Cape Basin (*16*), while nevertheless remaining on the deep-water "umbilicus" that links the Atlantic with the immense Indo-Pacific.

The chronology for core MD07-3076 is based on 59 monospecific planktonic foraminifer accelerator mass spectrometry (AMS) $^{14}C$ dates that have been corrected for variable reservoir age effects. We applied two independent methods to constrain local reservoir age variability. First, Antarctic ice-core ages obtained via correlation of Antarctic and local sea-surface temperature trends (fig. S3) were used to derive reservoir age ranges at stratigraphic tie-points (*15*). These estimates were verified against surface reservoir ages that were inferred independently from the published chronology for core TNO57-21 (Cape Basin) (*3*). Both methods yield strikingly similar histories of reservoir age variability at the site of MD07-3076, with a large increase in surface reservoir ages occurring during HS1 in particular. Reservoir ages at the more southerly site of MD07-3076 exceed those in the Cape Basin by ~2000 years, suggesting the northward migration of the sub-Antarctic Front (and divergence) to a position between the two cores. We derived age-depth models for multiple reservoir age scenarios using the Bayesian calibration and age-modeling program *Bchron* (*17*), providing a bounded "best estimate" reservoir age scenario and chronology that uses all available chronostratigraphic constraints (ice core and marine). The resulting chronology possesses quantifiable uncertainties and is in good agreement with two independent age scales (fig. S8).

The reconstructed deep-water ventilation/reservoir age history from core MD07-3076 is illustrated in Fig. 2D [benthic-planktonic age offsets (B-P)] and Fig. 2E [benthic-atmospheric age offsets (B-Atm)]. As shown in Fig. 2, D and E, deep water in the Atlantic sector of the Southern Ocean was poorly ventilated during the last glacial period, before HS1, reaching on average ~1630 years older than the local sea surface (B-P) and 2000 to 3750 years older than the atmosphere (B-Atm). This represents an increase of between 1.6 and 3 times relative to the modern ventilation ages (modern B-P is ~550 years, and modern B-Atm is ~1250 years) (Fig. 2, D and E). During the last glacial period, and at the Last Glacial Maximum (LGM) in particular, the time scale of carbon exchange between the atmosphere and the deep Southern Ocean therefore appears to have exceeded that of the most poorly ventilated regions of the modern deep North Pacific. All else being equal, this increase in the ventilation time scale of the deep sea would have enhanced the carbon sequestration capacity of the deep ocean during the last glacial period, thus helping to reduce atmospheric $CO_2$.

Across the deglaciation, between the LGM and the end of the Pre-Boreal/Younger Dryas (PB-YD), the influence of exceptionally aged deep water gradually decreased at the location of MD07-3076 (Fig. 2E). This long-term trend toward better-ventilated deep water occurred in parallel with a general trend toward increased atmospheric $CO_2$ (Fig. 2A), a gradual reduction in Antarctic sea-ice production (Fig. 2B), and generally more negative but increasing atmospheric $\partial^{13}CO_2$ (Fig. 2C) (*18*). This time interval also coincides with a broad $\partial^{13}C$ "minimum" recorded by planktonic foraminifera in the Eastern Equatorial Pacific (EEP), which has been interpreted to reflect a combination of increased upwelling at low latitudes and increased remineralized nutrient export from the Southern Ocean (*19*, *20*). All of these records are consistent, with a "mode shift" in the exchange of $CO_2$ between the ocean interior and the atmosphere across the last deglaciation, resulting in a tendency for greater exchange between the atmosphere and a marine carbon pool (*18*) that was especially depleted in $\partial^{13}C$ (*19*, *21*) and $\Delta^{14}C$ (Figs. 1A and 2D).

However, closer inspection of Fig. 2 also reveals that the deglacial trends in $CO_2$, Antarctic

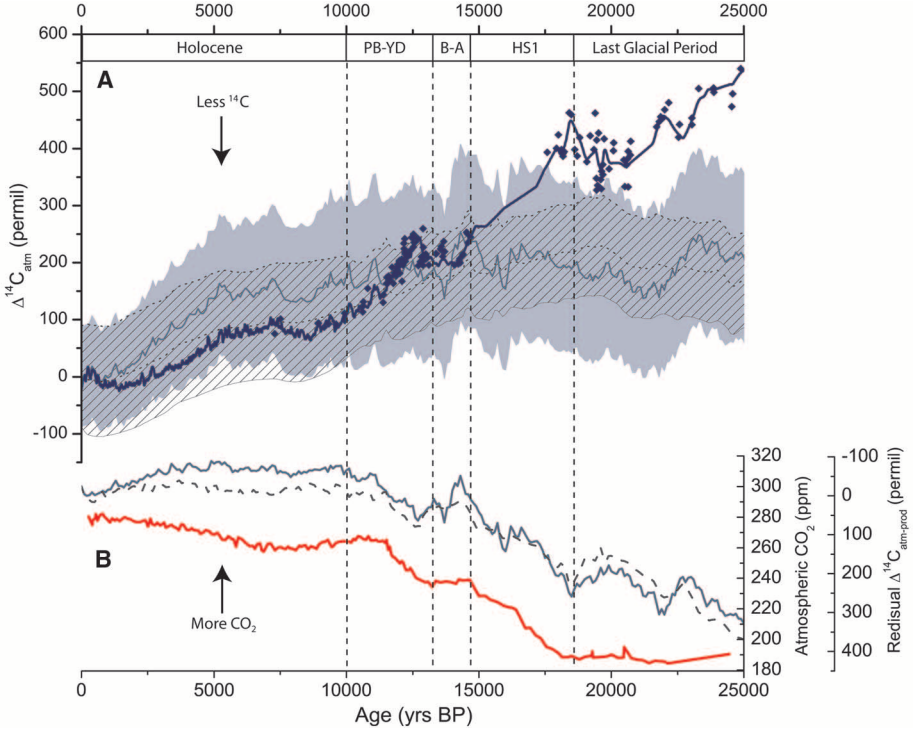


**Fig. 1.** Atmospheric $CO_2$ and radiocarbon activity ($\Delta^{14}C$) changes across the last deglaciation. (**A**) Reconstructed atmospheric $\Delta^{14}C$ [blue diamonds indicate coral data (*22*), and the blue line is the INTCAL04 calibration curve (*23*)], compared with the expected atmospheric $\Delta^{14}C$ record based only on $^{14}C$-production changes, derived using the BICYCLE model (*24*) with constant modern carbon cycling, and upper and lower $^{14}C$ production limits from Greenland ice-core $^{10}Be$ fluxes (shaded area) (*25*) and global paleomagnetic field intensity (hatched area) (*26*). (**B**) Atmospheric $CO_2$ concentrations from the European Project for Ice Coring in Antarctica (EPICA) Dome C (EDC) ice core (red line) (*10*), including one $CO_2$ measurement at 24.4 ky B.P. from the Taylor Dome ice core (*27*). The $CO_2$ data are shown here on EDML-GICC05 equivalent ages (*15*). The gray and blue lines in (B) indicate the difference between the reconstructed $\Delta^{14}C_{atm}$ record and the median simulated production histories from paleomagnetic intensity (dashed gray line) and $^{10}Be$ fluxes (solid blue line). These lines indicate atmospheric $\Delta^{14}C$ changes that may be attributed to carbon cycle changes (indicated with the inverted *y* axis). Vertical lines bound two rapid drops in atmospheric $\Delta^{14}C$, which do not coincide with similar changes in $^{14}C$-production but do coincide with rapid jumps in $CO_2$. These intervals are roughly coincident with HS1 and the YD, as indicated by the chronostratigraphic labels at the top of the graph. BA, Bølling-Allerød.

sea ice, atmospheric $\partial^{13}CO_2$, and deep-water ventilation were not monotonic. During the Antarctic Cold Reversal (ACR)/Bølling-Allerød, $CO_2$ (Fig. 2A) and $\partial^{13}CO_2$ (Fig. 2C) reversed their increasing trends, whereas $\Delta^{14}C_{atm}$ paused in its rapid decline (Fig. 1). In order to explain why these changes may have occurred, we identify three sets of conditions: (i) LGM, maximally extended Antarctic sea ice in conjunction with exceptionally aged circumpolar deep water (CDW) and stable but low $CO_2$; (ii) HS1 and YD, receding Antarctic sea ice in conjunction with relatively aged CDW and rising $CO_2$; and (iii) ACR/Bølling-Allerød, reduced but expanding Antarctic sea ice in conjunction with very young CDW and more elevated but approximately stable $CO_2$.

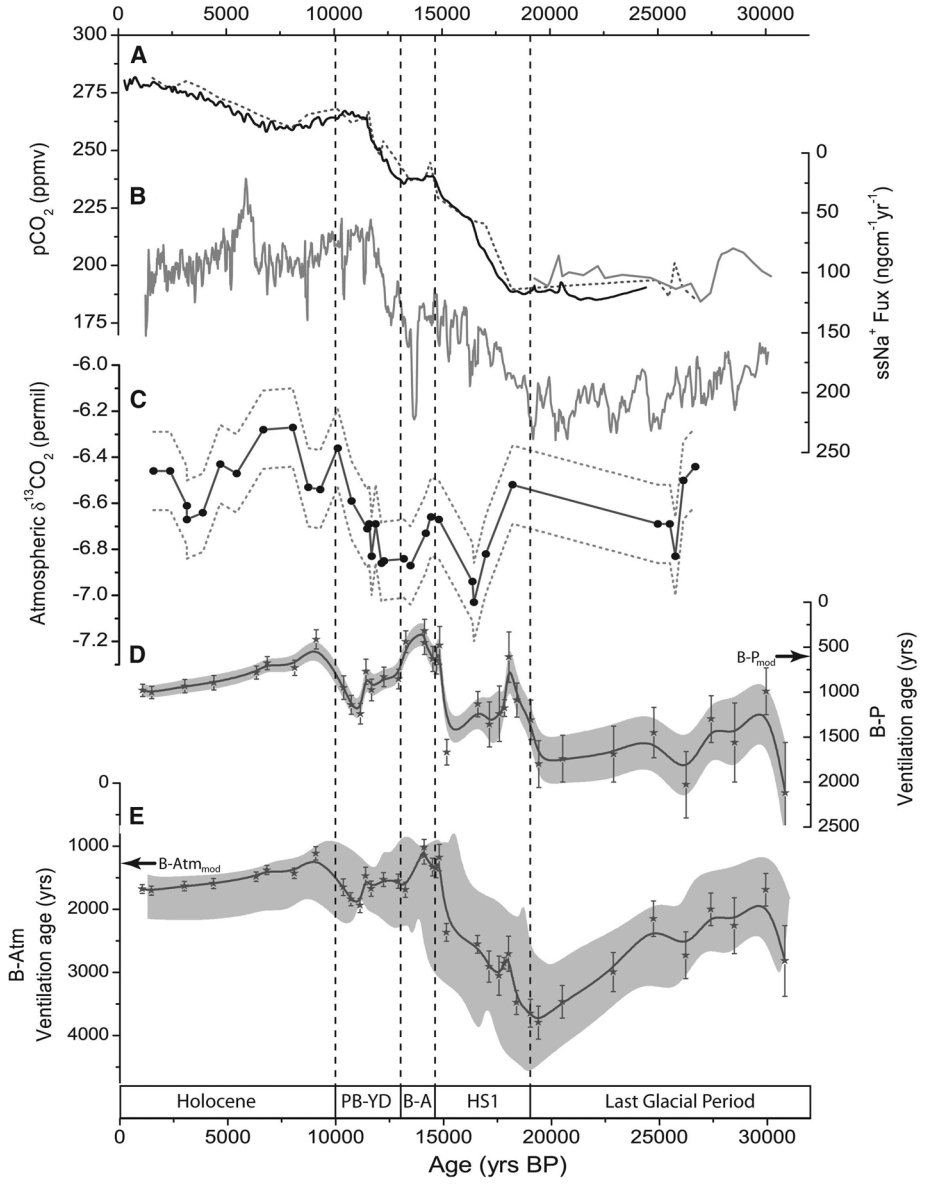


**Fig. 2.** Deep-water ventilation changes in the Atlantic sector of the Southern Ocean. (**A**) Atmospheric $CO_2$ from the EDC (*10*), Taylor Dome (*18*), and Byrd (*5*) ice cores, shown by solid dark gray, dashed, and light gray lines, respectively, and placed on the age scale of (*28*). (**B**) Sea salt–derived sodium fluxes from the EPICA Dronning Maud Land (EDML) ice core (*29*), as a regional sea-ice proxy, also on the NGRIP-GICC05 age scale. Although this is only an indirect sea ice proxy, it shows a deglacial pattern that is qualitatively similar to other marine proxy–based reconstructions. (**C**) $\partial^{13}CO_2$ measurements from the Taylor Dome Antarctic ice core (*18*), placed on the NGRIP-GICC05 age scale by alignment of $CH_4$ trends (*15*). Dotted lines indicate 2σ uncertainty range. (**D**) Benthic-planktonic $^{14}C$ age offsets in core MD07-3076 (error bars represent combined 1σ error in $^{14}C$ dates; shaded area indicates b-spline smoothed upper/lower limits of B-P defined by the 1σ error bars). (**E**) Apparent deep-water ventilation in core MD07-3076 (B-Atm). Heavy gray line (b-spline smoothed) and stars indicate the best estimate ventilation history and associated chronology. Vertical error ranges show the magnitude of combined planktonic/benthic $^{14}C$ date uncertainties (1σ). The shaded area shows the range of ventilation histories (b-spline smoothed) that could be supported by alternative surface reservoir age scenarios. Labels at the base indicate approximate timing of North Atlantic event-stratigraphy chronozones.

The associations identified above are consistent with the idea that the retraction of Antarctic sea ice from its maximal LGM extent may have increased the latitude band over which westerly winds could "stir up" CDW along steepened isopycnals, which would now outcrop increasingly to the south. This process may have been exacerbated during North Atlantic stadials (HS1 and the YD) because of an increase in the southward heat transport of the South Atlantic gyre via the "bipolar seesaw" mechanism (*2*, *3*). Although the CDW being brought to the surface in this way remained under the influence of an exceptionally aged and presumably high-potential partial pressure of $CO_2$ ($P_{CO_2}$) abyssal reservoir (water that would have high $P_{CO_2}$ when brought to the sea surface), the rate of $CO_2$ release from the Southern Ocean would have been enhanced (such as during HS1 and the YD) (Fig. 2, D and E). On the other hand, when the CDW that was being brought to the surface came under the influence of much better ventilated and presumably lower potential $P_{CO_2}$ deep water, as it did during the ACR/Bølling-Allerød (Fig. 2, D and E), the release of $CO_2$ from the Southern Ocean would have been much reduced.

The drop in ventilation ages observed in MD07-3076 approximately in time with the ACR/Bølling-Allerød (Fig. 2E) is coherent with similar features observed in the Pacific (*11*, *14*) and North Atlantic (*9*, *13*). This is shown in Fig. 3, which compares the evolution of atmospheric $\Delta^{14}C_{atm}$ with ventilation changes reconstructed for the deep Southern Ocean [MD07-3076 (this study)], the shallow east Pacific [GCMV99-GC31/PC08 (*11*)], and the deep Northeast Atlantic [MD99-2334K (*13*), supplemented here with three additional benthic $^{14}C$ dates (*15*)]. This comparison suggests that the exceptionally aged deep water that is thought to have escaped into the shallow Pacific via Antarctic Intermediate Water (AAIW) during HS1 and the YD (*11*), and that is also inferred to have been mixed into the North Atlantic at these times (*9*, *13*), was previously restricted to the deep Southern Ocean where it increasingly influenced the site of MD07-3076 as the LGM approached. It would also appear that despite its proximity to this exceptionally aged water mass, the site of MD07-3076 apparently was not (or did not remain) at its core. This is implied by the increase in ventilation ages in MD07-3076 toward the LGM and by the much higher ventilation ages observed at the shallow Pacific site between the middle of HS1 and the end of the YD (~16 to 10 ky B.P., Fig. 3B). Assuming that the shallow Pacific site is indeed representative of southern sourced water, the reversal in ventilation gradient between the two marine sites could suggest that the aged abyssal reservoir remained partially intact somewhere in the abyss until the end of the YD, despite having substantially withdrawn from the Atlantic sector of the deep Southern Ocean by this time (Fig. 2E).

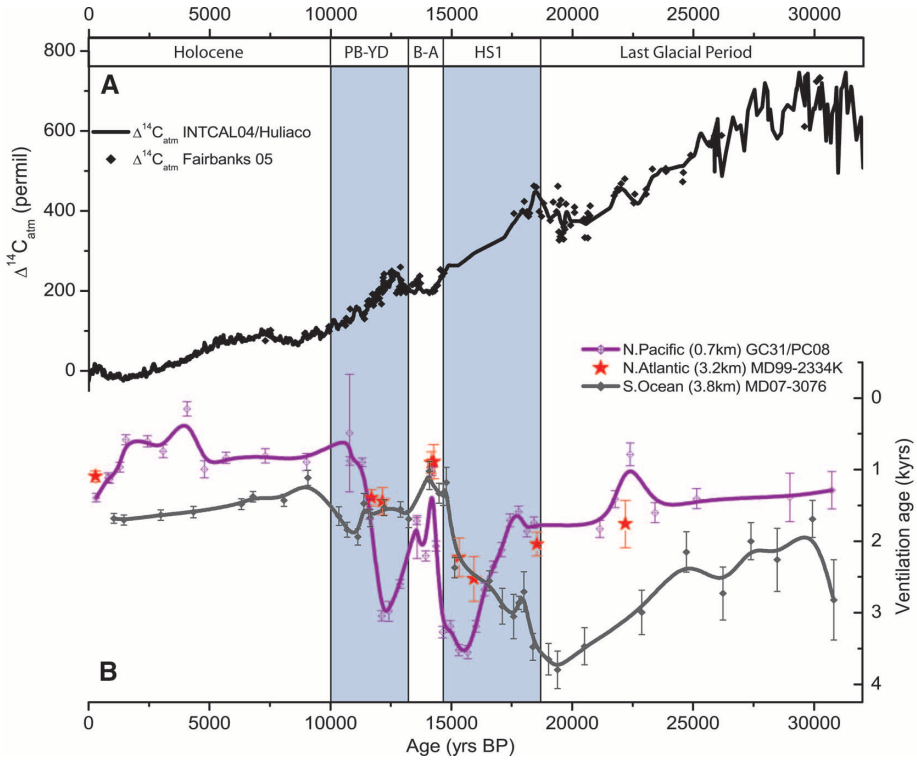


**Fig. 3.** Atmospheric $\Delta^{14}C$ change and deep-water reservoir age variability in the shallow Pacific, deep North Atlantic (*13*, *15*), and the deep Southern Ocean (this study). (**A**) Atmospheric $\Delta^{14}C$ [black diamonds, coral data (*22*); black line, INTCAL04 calibration curve (*23*) spliced with the Cariaco data set from 26 ky B.P. (*7*)]. (**B**) Deep water reservoir ages, derived from the offset between benthic- and atmospheric-$^{14}C$ ages (reversed *y* axis). Solid red stars indicate MD99-2334K from the deep Northeast Atlantic (*13*), purple crossed diamonds and b-spline smoothed line indicate GCMV99-GC31/PC08 from the shallow Pacific (*11*), and gray diamonds and b-spline smoothed indicate MD07-3076 from the Southern Ocean (this study). Error ranges for MD99-2334K and MD07-3076 indicate combined planktic and benthic $^{14}C$ age uncertainties (1σ), whereas those for GCMV99-GC31/PC08 are 2σ uncertainties in benthic $^{14}C$ ages alone (Fig. 2E). Shaded vertical bars highlight the coincidence of rapid changes in deep water ventilation with marked changes in $\Delta^{14}C_{atm}$ and major North Atlantic chronozones.

One important question that arises concerns the extent to which the changes in deep-water ventilation recorded in MD07-3076 help to explain the apparent glacial $\Delta^{14}C_{atm}$ excess and the rapid 190 per mil (‰) drop in $\Delta^{14}C_{atm}$ during HS1 (*8*) (Fig. 1). Answering this question accurately would require knowledge of the exact volume of deep water that was affected by the ventilation changes recorded at the site of MD07-3076. Without this knowledge, we can only say that if the ~2000-year reduction in B-Atm recorded across HS1 in MD07-3076 (Fig. 2E) was experienced by ~30% of the ocean [all water deeper than the next deepest $^{14}C$ constraint from the glacial Pacific (*12*)], this could explain just over half of the 190‰ drop in atmospheric $\Delta^{14}C$ across the mystery interval (*15*). At the very least, this provides cause for optimism regarding the eventual reconciliation of the deglacial "radiocarbon mystery" (*8*), though it also underlines the need for a wider array of deep-ocean $^{14}C$ data with precise calendar chronologies.

The cause of the transient increase in ventilation recorded during the ACR/Bølling-Allerød in MD07-3076 [and in other records from the Atlantic and Pacific (Fig. 3B)] is also difficult to assess accurately without knowledge of the changing "end-member" composition and mixing ratio of local deep water. Neodymium isotope data from core RC11-83 in the deep Cape Basin (*16*) suggests a variable but generally increased influence of northern-sourced deep water during the ACR/Bølling-Allerød relative to the LGM, but crucially not relative to the late Holocene. If this record is taken as representative of end-member mixing ratio changes at our more open Atlantic site, it follows that mixing ratio changes alone might

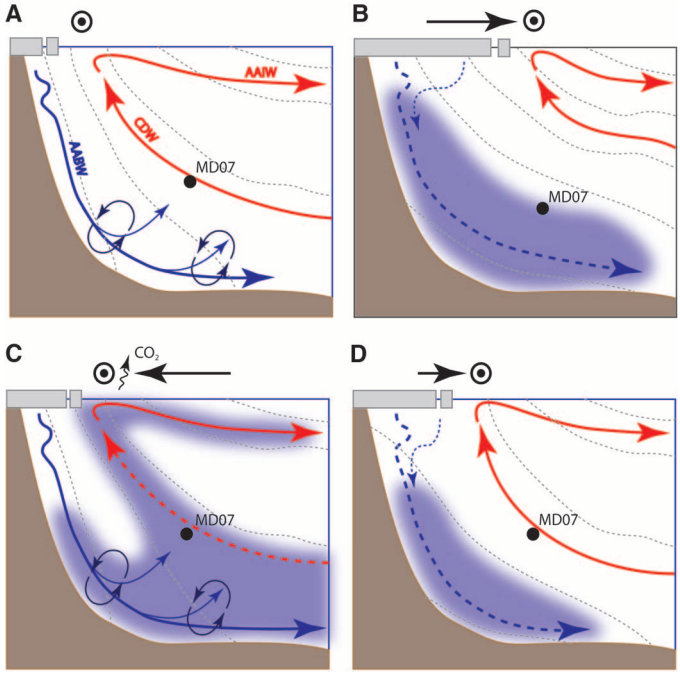


**Fig. 4.** Schematic illustration of hypothesized changes in Southern Ocean overturning across the last deglaciation (with south at left). (**A**) The modern overturning. Red arrows indicate the "upper overturning limb," which here includes CDW upwelling in the Southern Ocean at the ACC divergence and AAIW flowing northwards at shallow depths. Upper and lower CDW, which may include North Atlantic– and Antarctic-sourced water in variable proportions, have been combined for simplicity. Blue arrows indicate the "lower overturning limb," which consists of Antarctic Bottom Water (AABW) and its derivatives. Gray dashed lines indicate hypothetical isopycnals. Dark blue circular arrows indicate intense diapycnal mixing around topography in the Southern Ocean, which permits effective lower-limb overturning and the incorporation of AABW into CDW (*15*). Sea ice is represented by the gray boxes (top left), and the westerly wind position is indicated by the dotted circle (top). The solid circle marks the approximate position of core MD07-3076. (**B**) LGM overturning. The North Atlantic (salt) contribution to the upper-limb circulation is subdued relative to the present; Antarctic sea ice and the effective westerly wind stress in the Southern Ocean (driving isopycnal outcropping) are pushed far northward (black arrow). Flattened and widely spaced isopycnals south of the main outcropping area cause the $^{14}C$-depleted lower overturning limb to expand without substantial diapcynal mixing into CDW. The shaded area indicates a $^{14}C$-depleted, high potential $Pco_2$ deep-water mass. (**C**) HS1/YD overturning. The supply of North Atlantic deep water to CDW is severely reduced, the Southern Ocean warms in part because of the bipolar seesaw, Antarctic sea ice retracts substantially from its maximum glacial extent, and the main isopycnal outcrop area shifts southward. Poorly ventilated (high potential $Pco_2$) AABW is drawn upward along steepened isopycnals and mixed to a greater extent into CDW, which releases $^{14}C$-depleted $CO_2$ to the atmosphere when brought to the surface. (**D**) Bølling-Allerød overturning. The Southern Ocean cools because of the bipolar seesaw, and sea ice reverses its retreat. Mixing of AABW into upward-flowing CDW is impeded once again, and the release of $^{14}C$-depleted $CO_2$ pauses as a result.

not account for near modern deep-water ventilation ages observed during the ACR/Bølling-Allerød (Fig. 2E). This would suggest that either the export rate or ocean-atmosphere equilibration of one or both of the main Atlantic deep-water end-members (North Atlantic and/or Antarctic) increased during the ACR/Bølling-Allerød.

Our results demonstrate the existence before HS1 of an exceptionally aged abyssal carbon reservoir that could have substantially contributed to the sequestration of $CO_2$ in the deep sea during the last glacial period. These results also underline the potential importance of the combined effects of changing Antarctic sea ice, wind forcing, and abyssal stratification on the deglacial rise of $CO_2$. As illustrated schematically in Fig. 4, we envisage that although the meridional extent of Antarctic sea ice should influence the efficacy of the westerly wind stress that can effectively be applied to the Antarctic Circumpolar Current (ACC) to drive the upwelling of the densest classes of CDW in the Southern Ocean, the impact of upwelling on atmospheric $CO_2$ ($\Delta^{14}C_{atm}$ and $\partial^{13}CO_2$) might ultimately be determined by changes in the potential $Pco_2$ and sequestration age of the CDW that is brought to the surface. Thus, the deglacial trends in atmospheric $CO_2$, $\partial^{13}CO_2$, and $\Delta^{14}C_{atm}$ may have been interrupted during the ACR/Bølling-Allerød at least partly as a result of a pronounced increase in the ventilation of CDW brought to the surface Southern Ocean at this time (Figs. 2D and 4D). In contrast, with the preponderance of exceptionally aged CDW during HS1 and the YD [and with Antarctic sea ice already pulled back from its maximal meridional extent (Fig. 4C)], high potential $Pco_2$ water would be brought to the surface Southern Ocean instead. The result would have been to greatly enhance the release of $^{14}C$-depleted $CO_2$ to the atmosphere, as well as the export of $^{14}C$-depleted water from the ACC to the Atlantic and Pacific at these times.

### References and Notes


1. W. Broecker, G. M. Henderson, *Paleoceanography* **13**, 352 (1998).
2. R. F. Anderson *et al.*, *Science* **323**, 1443 (2009).
3. S. Barker *et al.*, *Nature* **457**, 1097 (2009).
4. U. Siegenthaler *et al.*, *Science* **310**, 1313 (2005).
5. J. Ahn, E. J. Brook, *Science* **322**, 83 (2008).
6. F. Primeau, *J. Phys. Oceanogr.* **35**, 545 (2005).
7. K. Hughen, J. Southon, S. Lehman, C. Bertrand, J. Turnbull, *Quat. Sci. Rev.* **25**, 3216 (2006).
8. W. Broecker, S. Barker, *Earth Planet. Sci. Lett.* **256**, 90 (2007).
9. L. F. Robinson *et al.*, *Science* **310**, 1469 (2005).
10. E. Monnin *et al.*, *Science* **291**, 112 (2001).
11. T. M. Marchitto, S. J. Lehman, J. D. Ortiz, J. Flückiger, A. van Geen, *Science* **316**, 1456 (2007).
12. W. Broecker, E. Clark, S. Barker, *Earth Planet. Sci. Lett.* **274**, 322 (2008).
13. L. C. Skinner, N. J. Shackleton, *Paleoceanography* **19**, PA2005 (2004).
14. E. D. Galbraith *et al.*, *Nature* **449**, 890 (2007).
15. Materials and methods are available as supporting material on *Science* Online.
16. A. M. Piotrowski, S. L. Goldstein, S. R. Hemming, R. G. Fairbanks, *Earth Planet. Sci. Lett.* **225**, 205 (2004).
17. A. C. Parnell, J. Haslett, J. R. M. Allen, C. E. Buck, B. Huntley, *Quat. Sci. Rev.* **27**, 1872 (2008).
18. H. J. Smith, H. Fischer, M. Wahlen, D. Mastroianni, B. Deck, *Nature* **400**, 248 (1999).
19. H. J. Spero, D. W. Lea, *Science* **296**, 522 (2002).
20. L. Pena, I. Cacho, P. Ferretti, M. A. Hall, *Paleoceanography* **23**, PA3101 (2008).
21. P. Kohler, H. Fischer, G. Munhoven, R. E. Zeebe, *Global Biogeochem. Cycles* **19**, GB4020 (2005).
22. R. G. Fairbanks *et al.*, *Quat. Sci. Rev.* **24**, 1781 (2005).
23. P. J. Reimer *et al.*, *Radiocarbon* **46**, 1029 (2004).
24. P. Kohler, R. Muscheler, H. Fischer, *Geochem. Geophys. Geosyst.* **7**, Q11N06 (2006).
25. R. Muscheler, J. Beer, P. W. Kubik, H.-A. Synal, *Quat. Sci. Rev.* **24**, 1849 (2005).
26. C. Laj, C. Kissel, J. Beer, in *Timescales of the Paleomagnetic Field*. (American Geophysical Union, 2004), vol. 145, pp. 255–265.
27. A. Indermuhle, E. Monnin, B. Stauffer, T. F. Stocker, M. Wahlen, *Geophys. Res. Lett.* **27**, 735 (2000).
28. B. Lemieux-Dudon *et al.*, *Quat. Sci. Rev.* **29**, 8 (2010).
29. H. Fischer *et al.*, *Earth Planet. Sci. Lett.* **260**, 340 (2007).


30. We are grateful to N. Caillon, F. Dewilde, G. Isguder, H. Rebaubier, L. Booth, P. Ljubic, and K. James for technical assistance. A. Parnell provided generous and invaluable help with *Bchron*, and P. Köhler very kindly provided unpublished $\Delta^{14}C_{atm}$ simulations. We thank R. Gersonde and A. Mackensen for sharing their South Atlantic expertise, and we acknowledge the crew of the R/V Marion Dufresne and the Paul Emile Victor Institute (IPEV) who collected core MD07-3076CQ. This work was funded by the Royal Society, by Natural Environment Research Council Radiocarbon grant 1245.1007, and via a University Fellowship held by L.C.S. This work was facilitated by a visiting fellowship held by L.C.S. at ANU and by travel grants from the Royal Society and Christ's College. C.W. and E.M. are supported financially by Centre National de la Recherche Scientifique, Institut National des Sciences de l'Univers, and Commissariat à l'Energie Atomique. This is Laboratoire des Sciences du Climat et l'Environnement contribution 4188.


### Supporting Online Material

www.sciencemag.org/cgi/content/full/328/5982/1147/DC1
Materials and Methods
Figs. S1 to S8
Tables S1 to S3
References

20 October 2009; accepted 8 April 2010
10.1126/science.1183627

# Mirid Bug Outbreaks in Multiple Crops Correlated with Wide-Scale Adoption of Bt Cotton in China

**Yanhui Lu,[1] Kongming Wu,[1]* Yuying Jiang,[2] Bing Xia,[2] Ping Li,[2] Hongqiang Feng,[1] Kris A. G. Wyckhuys,[1]† Yuyuan Guo[1]**

Long-term ecological effects of transgenic *Bacillus thuringiensis* (Bt) crops on nontarget pests have received limited attention, more so in diverse small holder–based cropping systems of the developing world. Field trials conducted over 10 years in northern China show that mirid bugs (Heteroptera: Miridae) have progressively increased population sizes and acquired pest status in cotton and multiple other crops, in association with a regional increase in Bt cotton adoption. More specifically, our analyses show that Bt cotton has become a source of mirid bugs and that their population increases are related to drops in insecticide use in this crop. Hence, alterations of pest management regimes in Bt cotton could be responsible for the appearance and subsequent spread of nontarget pests at an agro-landscape level.

Genetically engineered crops that express δ-endotoxins (Cry proteins) from *Bacillus thuringiensis* (Bt) can successfully control several insect pests. The adoption of Bt crops increases yield and causes vast reductions in insecticide use (*1*–*5*). With Bt crops presently adopted in over 20 countries (*6*), the ecological risks of their commercial cultivation have received considerable scientific scrutiny (*7*–*11*). In China, Bt cotton was approved in 1997 for commercial use to control cotton bollworm, *Helicoverpa armigera*, and has steadily been adopted by the bulk of Chinese cotton growers (i.e., presently 95% adoption in northern China). Bt cotton controls *H. armigera* larvae very effectively and acts as a dead-end trap crop for regional populations of this pest in local agricultural landscapes (*12*); that is, a large percentage of the pest moths lay their eggs in cotton, where the hatching larvae are killed and do not subsequently infest other crops as adults. Hence, Bt cotton controls a key target pest not only within cotton fields but also on multiple other non-Bt host crops (i.e., corn, peanuts, soybeans, and vegetables), reducing the overall need for insecticide sprays (*3*, *12*). Nevertheless, long-term impacts of Bt cotton on nontarget arthropods, such as polyphagous insect pests, in local agro-ecosystems remain to be quantified (*13*–*15*).

Mirid bugs (Heteroptera: Miridae) are herbivores in a broad range of cultivated plants, including

[1]State Key Laboratory for Biology of Plant Diseases and Insect Pests, Institute of Plant Protection, Chinese Academy of Agricultural Sciences, Beijing 100193, People's Republic of China. [2]National Agro-Technical Extension and Service Center, Beijing 100026, People's Republic of China.

*To whom correspondence should be addressed. E-mail: kmwu@ippcaas.cn

†Present address: Horticulture Research Center, Universidad Jorge Tadeo Lozano, Chia (Cundinamarca), Colombia.